Chapter 2

Phospholipid Interaction Sites of α-Synuclein Determined by Tryptophan

2.1 ABSTRACT

A hallmark of Parkinson's disease is the presence of fibrillar α-synuclein deposits in the brain. Although its function is ill defined, α-synuclein is found to associate with synaptic vesicles. Interestingly, α-synuclein appears to be natively unfolded *in vitro*. However, in the presence of membrane mimics (e.g., SDS micelles and acidic phospholipid vesicles), the protein adopts a highly helical conformation. We have prepared six single tryptophan-containing variants (W4, W39, W94, W101, W125, and W136). Their interactions with phospholipid vesicles by steady-state and time-resolved fluorescence measurements were probed. Using energy-transfer (dinitrophenol) and heavy-atom (bromine) labeled phospholipids, the relative location of the different Trp residues in the bilayer was determined to be on the order of W4>>W94>W39>W101>W136≥W125, from buried to water exposed.

2.2 INTRODUCTION

Though α-syn is characterized to be unstructured *in vitro*,[1] numerous experimental data now indicate that α-syn is not a random coil, but contains regions of structural preferences.[2-7] In the presence of acidic phospholipid vesicles, the protein will adopt α-helical structures. Notably, α-syn does not appear to interact with neutral phospholipid vesicles.[8] These structures have been characterized by circular dichroism (CD),[9] nuclear magnetic resonance (NMR),[10-12] and electron paramagnetic resonance (EPR) spectroscopies.[13,14]

Previously, Ulmer et al.[15] have investigated the structure of α-syn in association with SDS micelles using NMR. Their results show that two α-helices are formed within the N-terminal region (residues 3-37 and 45-92) in an antiparallel arrangement, joined by a short linker (residues 38-44). The C-terminal tail remains unstructured. In a separate study, Langen and coworkers[14] have characterized the location of residues 8-89 when associated with small unilammelar vesicles (SUVs) using site-directed spin labeling. In contrast to the micellar bound conformer, each eleven-residue repeat folds into three α-helical turns. This arrangement can be attributed to the charge distribution of the amino acids within the repeats: the negatively charged residues are solvent exposed, alanine and valine residues are lipid exposed, and lysine residues are localized near the polar head group. Although a short linker also is observed when α-syn is associated with the vesicles, it does not arrange the helices in an antiparallel fashion.

In this study, measurements of steady-state and time-resolved fluorescence were employed to characterize the interactions of SUVs with α-syn. A single tryptophan mutation was incorporated into six different sites (W4, W39, W94, W101, W125, and W136) to serve as a fluorescent probe for distinct regions of the protein: W4 on the N-terminus, W39 in the linker region, W94 on the C-terminal end of the NAC sequence, W101, W125, and W136 in the highly acidic C-terminus. In addition, we utilized commercially available phospholipids containing heavy-atom (Br) and energy-transfer (dinitrophenol) quenchers to elucidate the specific location of the individual Trp residues with respect to the lipid bilayer.

2.3 METHODS

Preparation of Small Unilamellar Vesicles (SUVs).

SUVs were prepared from a 1:1 molar mixture of lipids, 1-palmitoyl-2-oleoyl-*sn*-glycero-3-phosphocholine (POPC), and 1-palmitoyl-2-oleoyl-*sn*-glycero-3-phosphate (POPA) following published protocols and was described in Chapter 1.[16] Brominated lipids chosen for this experiment were 1-palmitoyl-2-stearoyl(6,7-dibromo)-*sn*-glycero-3-phosphocholine (6,7-DiBr) and 1-palmitoyl-2-stearoyl(11,12-dibromo)-*sn*-glycero-3-phosphocholine (11,12-DiBr); mixed vesicles were made in a 1:2:1 molar ratio of POPC:POPA:Di-Br. The distances between the headgroup/hydrocarbon boundary and the bromine atoms were 3.5 Å and 8.0 Å, respectively.[17] The lipid labeled with an energy-transfer quencher, N-dinitrophenyl

phosphatidylethanolamine (DNP), located at the head group, were used in a molar ratio of 4:5:1 POPC:POPA:DNP.

Protein Preparation, Modification, and Characterization.

The protein preparation, modification, and characterization processes were described in Chapter 1. Site-directed mutagenesis was performed to introduce tryptophan at six different sites (W4, W39, W94, W101, W125, and W136). All mutated sequences were confirmed by DNA sequencing (California Institute of Technology DNA Sequencing Core Facility).

Steady-state Absorption and Fluorescence Spectroscopy.

Using gel filtration chromatography (PD-10 desalting columns, GE Healthcare), all purified protein samples were exchanged into 20 mM NaP_i (pH 7.4) for the N-terminal tail mutants or 10 mM HEPES (pH 7.4) for the C-terminal tail mutants. Buffer solutions were filtered through a 0.22-μm filter to remove any particulates, while stock protein solutions were filtered through Microcon YM-100 (MWCO 100 kD) (Millipore) spin filter units to ensure removal of oligomeric species before diluting into prepared SUVs. All samples contained 5 μM of protein with 1.4 mg/mL of SUVs. For the N-terminal tail mutants, measurements were made with proteins in buffer, POPC:POPA, and SUVs with the three types of different quenchers. Since it has been suggested not to insert the C-terminal tail into the membrane, the SUVs with Br(11,12)-POPC incorporated were not utilized.

To evaluate the amount of quenching for α-syn mutants in 25% 6,7-DiBr and 25% 11,12-DiBr SUVs, the ratios of quenched-to-unquenched emission (F/F_0) were calculated. Emissions were integrated between 300 nm and 500 nm after background substrations. The ratio was then obtained by comparing the integrated emissions of α-syn mutants between brominated SUVs and quencher-free SUVs.

Time-resolved Fluorescence Measurements.

Time-resolved fluorescence decay experiments were carried out as previously described in Chapter 1. For anisotropy decay kinetics measurements, samples were excited by a vertically polarized laser pulse and both polarizations (I_{VV} and I_{VH}) were collected simultaneously for each sample.

Data Analysis.

The measured fluorescence decay kinetics were fitted by previously described procedures.[5] Kinetics traces were logarithmically compressed (100 points per time decade) and modeled with NNLS fitting protocol to project the narrowest *P(k)* distributions from the fluorescence kinetics.[4] To provide more information on the amount of quenching for α-syn mutants in SUVs containing brominated lipids, quenched-to-unquenched lifetime ratio (τ/τ_0) was also determined by comparing their weighed fluorescent decay rate.

To calculate time-resolved anisotropy decay kinetics, the ratio of sensitivities (G) for the vertically and horizontally polarized light in the system is assumed to be one. However, all luminescence spectra were adjusted according to the I_{VV} and I_{VH}

luminescence spectra obtained from NATA. Then, the anisotropy value (r) could be obtained by applying this equation,

$$r = \frac{I_{VV} - GI_{VH}}{I_{VV} + 2GI_{VH}}.$$

The anisotropy decay curve was then fitted against single exponential decay to determine the rotational correlation time of each mutant in POPC:POPA SUVs.

2.4 RESULTS AND DISCUSSIONS

Steady-state Fluorescence.

Tryptophan emission is an extremely sensitive probe of protein local environments.[20-23] Shown in **Figure 2.1** and **Table 2.1** are the fluorescence properties of Trp mutants in NaP_i buffer and when bound to SUVs (1:1 POPC:POPA). For the model complex, NATA, and the C-terminal mutants, the Stokes shifts (59 nm) are similar for both buffer and vesicle solutions. These shifts are characteristic of a completely water-exposed indole (**Figure 2.1**). In contrast, the three N-terminal α-syn variants exhibit smaller Stokes shifts upon the addition of vesicles, revealing that the three Trp residues are located in more hydrophobic environments, while the C-terminal mutants remain in hydrophilic environments.

Among the three N-terminal mutants, W4 has the most pronounced blue-shifted emission (λ_{max} = 326 nm), suggesting that it is protected from water and embedded in the lipid bilayer. On the other hand, a lower quantum yield and a less blue-shifted peak for W94 demonstrates that this indole side chain is located in a less hydrophobic environment, likely closer to the polar phospholipid headgroups. The

	λ_{max} (nm)	
	20 mM NaP_i	1:1 POPC:POPA
NATA	354	353
W4	348	326
W39	348	340
W94	351	335
W101	348	352
W125	349	353
W136	346	352

Table 2.1. Fluorescence maxima of NATA and α-syn mutants in the presence of NaP_i and 1:1 POPC:POPA vesicles

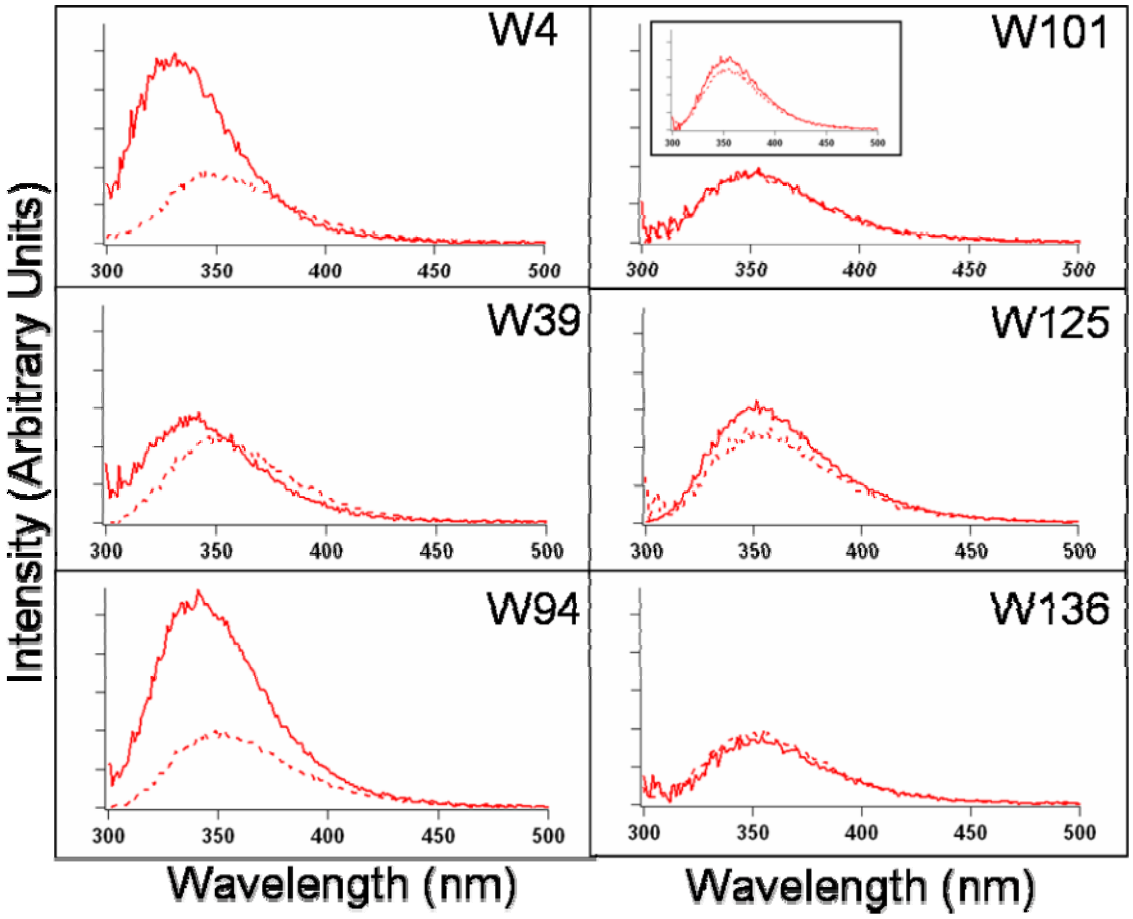

Figure 2.1. Steady-state fluorescence spectra of NATA (inset), W4 (top-left panel), W39 (middle-left panel), W94 (bottom-left panel), W101 (top-right panel), W125 (middle-right panel), and W136 (bottom-right panel) α-syn mutants in the presence of NaP_i (dotted) and 1:1 POPC:POPA vesicles (solid)

W39 protein exhibits the smallest quantum yield, suggesting that this residue is located closest to the surface of the SUV.

Using SUVs containing brominated lipids, distances between Trp and bromine quencher can be extrapolated empirically according to the degree of quenching by the bromine atoms.[24] W39 shows modest amount of quenching (< 10%) in the presence of the heavy atoms (**Table 2.2**), indicating that the tryptophan residue is at least > 14 Å away from both sites (6,7- and 11,12-DiBr, structures are shown in **Figure 1.2**). In contrast, nearly complete quenching (> 90% with 6,7- and ~ 40% with 11,12-Di-Br) is observed for the N-terminal W4, indicating that this indole is the most deeply inserted side-chain amongst the fluorophores.

For the C-terminal mutants, only 6,7-DiBr SUVs were examined because W101 and W136 showed minor quenching (< 10%) in the presence of the brominated lipids, while W125 fluorescence is unaffected. This agrees closely to previously published data that suggest that the C-terminal fragment is not involved in membrane binding.[11-14,25,26] However, our results reveal that W101 and W136 may be located closer to the membrane than W125.

To further map out the Trp locations with respect to the polar headgroup, we utilized a phospholipid labeled with an energy acceptor moiety, dinitrophenol (λ_{abs} = 350 nm) in the headgroup. For all the mutants studied (W4, W39, W94, W101, W125, and W136), a high degree of tryptophan quenching was observed in the presence of the dinitrophenol group, attributable to inner filter effect of the energy-transfer quencher (data not shown). To eliminate the inner filter effects ($\varepsilon_{350\ nm}$ (DNP) = 13,353 $M^{-1}cm^{-1}$; OD > 2 at 10% DNP), time-resolved fluorescence decay kinetics

		F/F_0	Trp-Br Distance (Å)	τ/τ_0
W4	25 % 6,7-DiBr	0.1	6	0.1
	25 % 11,12-DiBr	0.6	11	0.2
W39	25 % 6,7-DiBr	0.8	> 14	0.9
	25 % 11,12-DiBr	0.9	> 14	1.0
W94	25 % 6,7-DiBr	0.6	11	0.2
	25 % 11,12-DiBr	0.7	14	0.4
W101	25 % 6,7-DiBr	0.9	> 14	0.8
W125	25 % 6,7-DiBr	1.0	> 14	0.9
W136	25 % 6,7-DiBr	0.9	> 14	0.9

Table 2.2. Ratios of quenched-to-unquenched emission (F/F_0), and quenched-to-unquenched lifetime (τ/τ_0) for α-syn mutants in 25% 6,7-DiBr and 25% 11,12-DiBr SUVs, and estimated distance between tryptophan and bromine atoms

measurements were required to assess the Trp→DNP quenching.

Time-resolved Fluorescence Kinetics.

To probe for phospholipid-protein interactions, Trp fluorescence decay kinetics were examined in the presence of 1:1 POPC:POPA vesicles (**Figure 2.2**). The fits extracted from non-negative linear least-squares (NNLS) analysis show that there are two dominant components, 3 x 10^{-9} s^{-1} (60%) and 1 x 10^{-9} s^{-1} (40%), for NATA in buffer. Indeed, all the α-syn mutants investigated show similar biexponential decays in the presence or absence of 1:1 POPC:POPA (**Figure 2.3 and Figure 2.4**).

Again, SUVs containing brominated lipids were used to determine the position of Trps when folded into the vesicles. The FET kinetics data were collected and fitted using the NNLS method (**Figure 2.5 and 2.6**). The degree of quenching (**Table 2.1**) can be evaluated by the quenched-to-unquenched ratio (τ/τ_0) of the Trp lifetimes. Conclusions on the relative location of Trps when inserted into the SUVs are similar to the predictions drawn from the steady state fluorescence studies.

Fitting the FET kinetics data in the presence of 10% DNP SUVs using the NNLS method can reveal the locations of tryptophan residues with respect to the surface of the vesicle. The appearance of ultra-fast lifetimes (< 0.1 ns) corresponds to energy transfer to the dinitrophenol group. The Förster distance between Trp-DNP is calculated to be 27.5 Å. The data indicate that W39 contains the highest subpopulation (~ 25%) of fast decay constants, while the N-terminal W4 has the least amount (~ 12%) (**Figure 2.7**). This result is consistent with our di-Br studies where

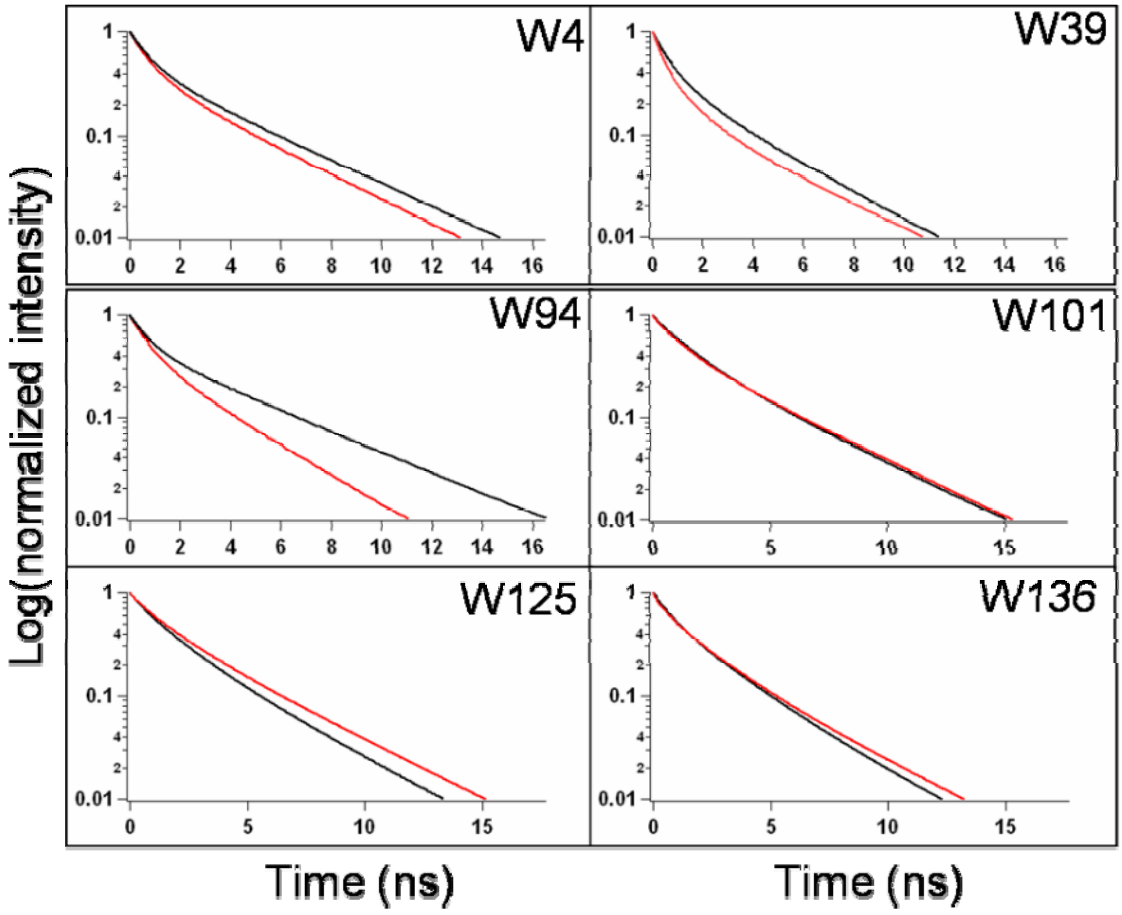

Figure 2.2. Time-resolved fluorescent kinetics of W4 (top left), W39 (top right), W94 (middle left), W101 (middle right), W125 (bottom left), and W136 (bottom right) α-syn mutants in 20 mM NaP_i buffer (red) and 1:1 POPC:POPA SUVs (black)

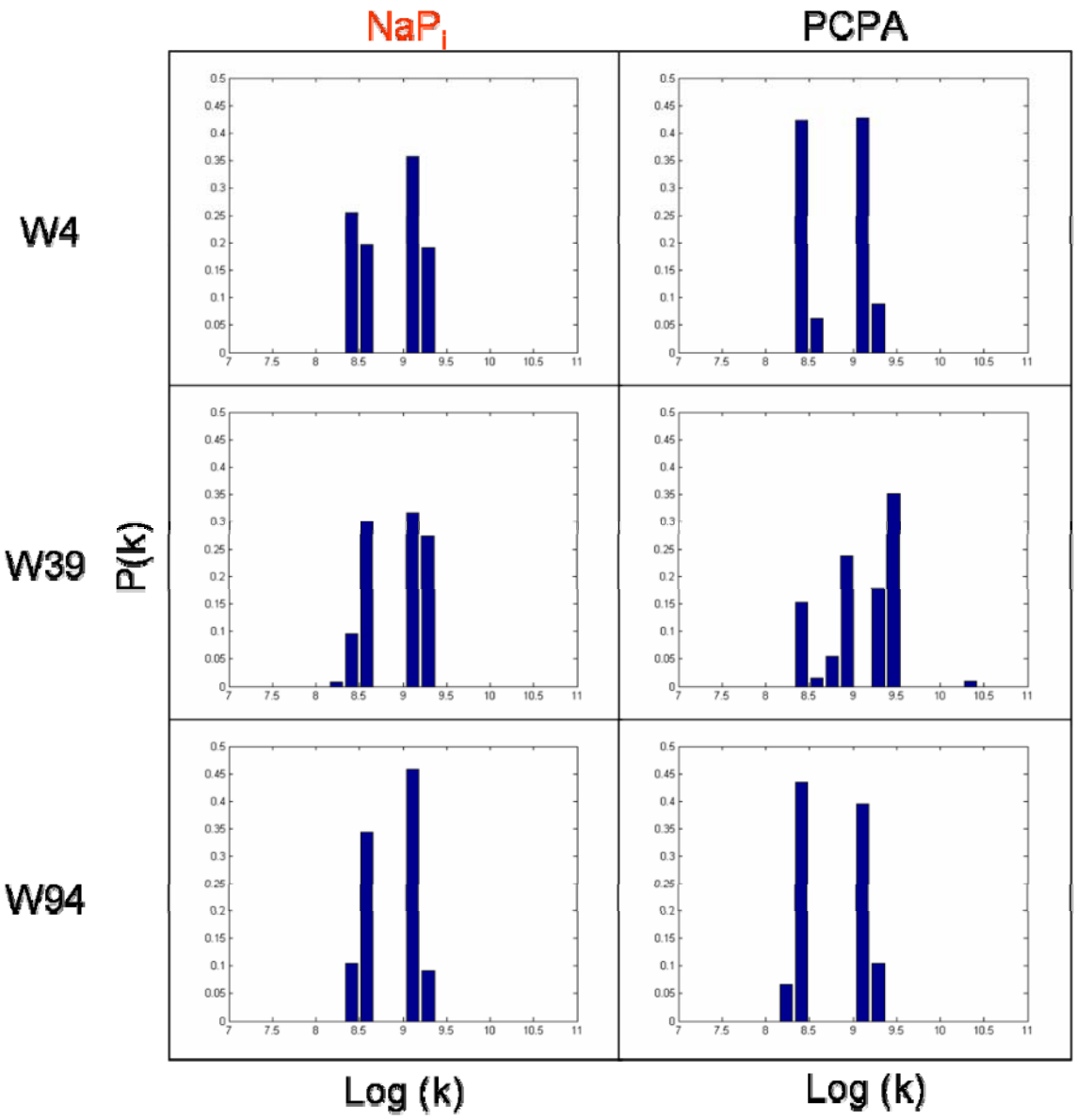

Figure 2.3. Distributions of tryptophan decay rate constants (k) for W4 (top), W39 (middle), and W94 (bottom) α-syn mutants in 20 mM NaP_i buffer (left) and 1:1 POPC:POPA SUVs (right)

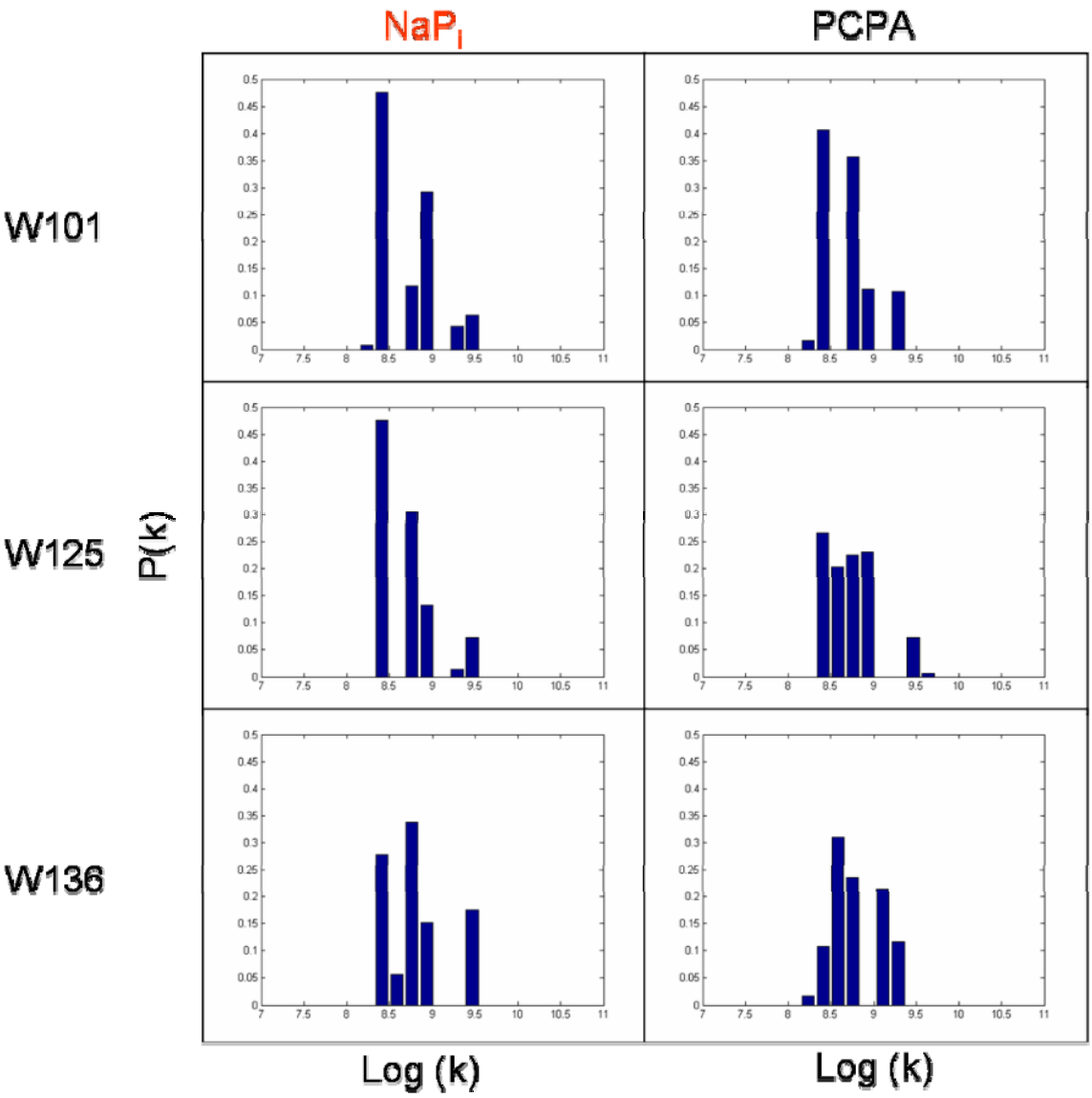

Figure 2.4. Distributions of tryptophan decay rate constants (k) for W101 (top), W125 (middle), and W136 (bottom) α-syn mutants in 20 mM NaP_i buffer (left) and 1:1 POPC:POPA SUVs (right)

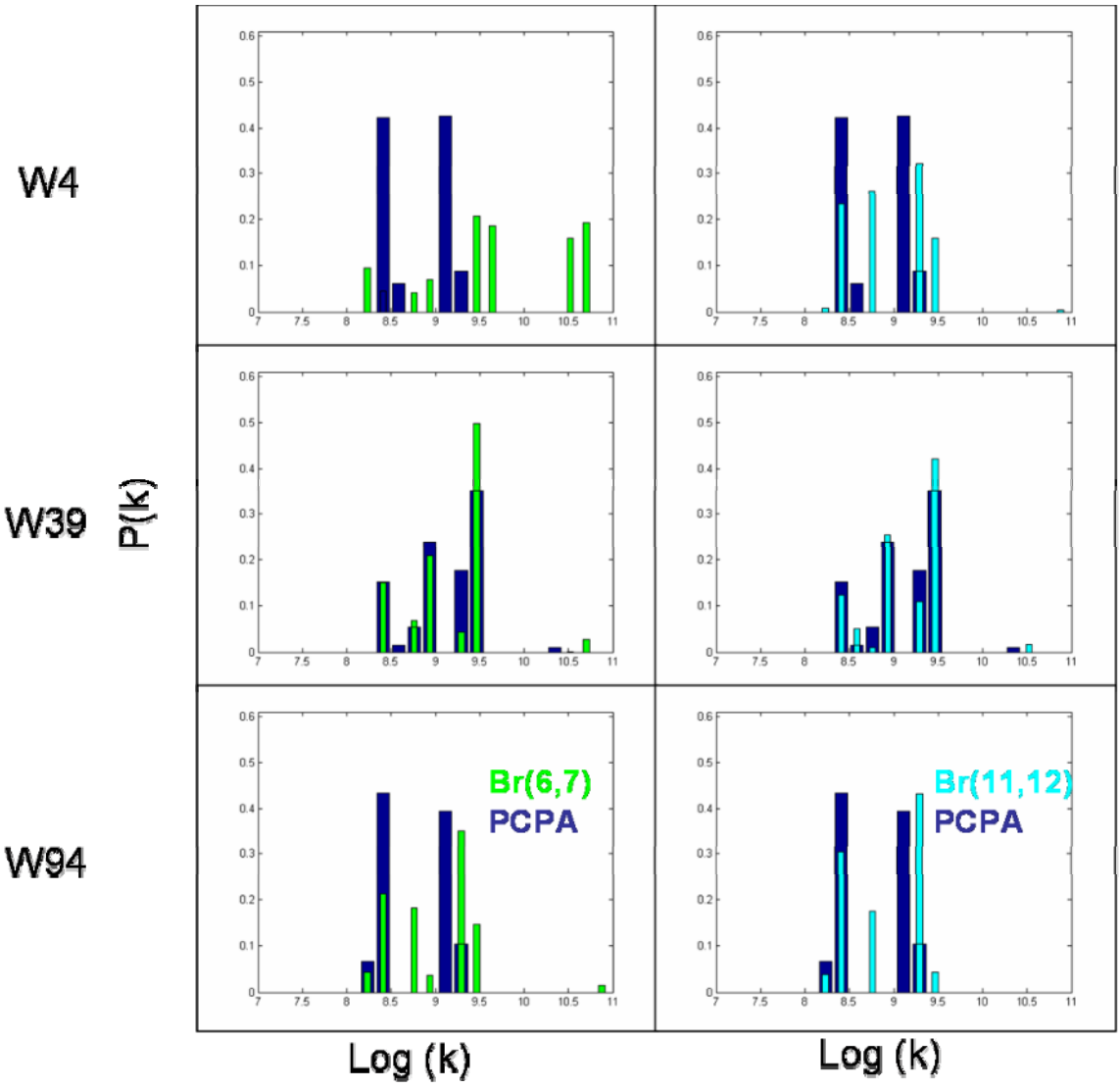

Figure 2.5. Distributions of tryptophan decay rate constants (k) for W4 (top), W39 (middle), and W94 (bottom) α-syn mutants in 1:1 POPC:POPA SUVs (dark blue), 6,7-DiBr SUVs (green), and 11,12-DiBr SUVs (aqua)

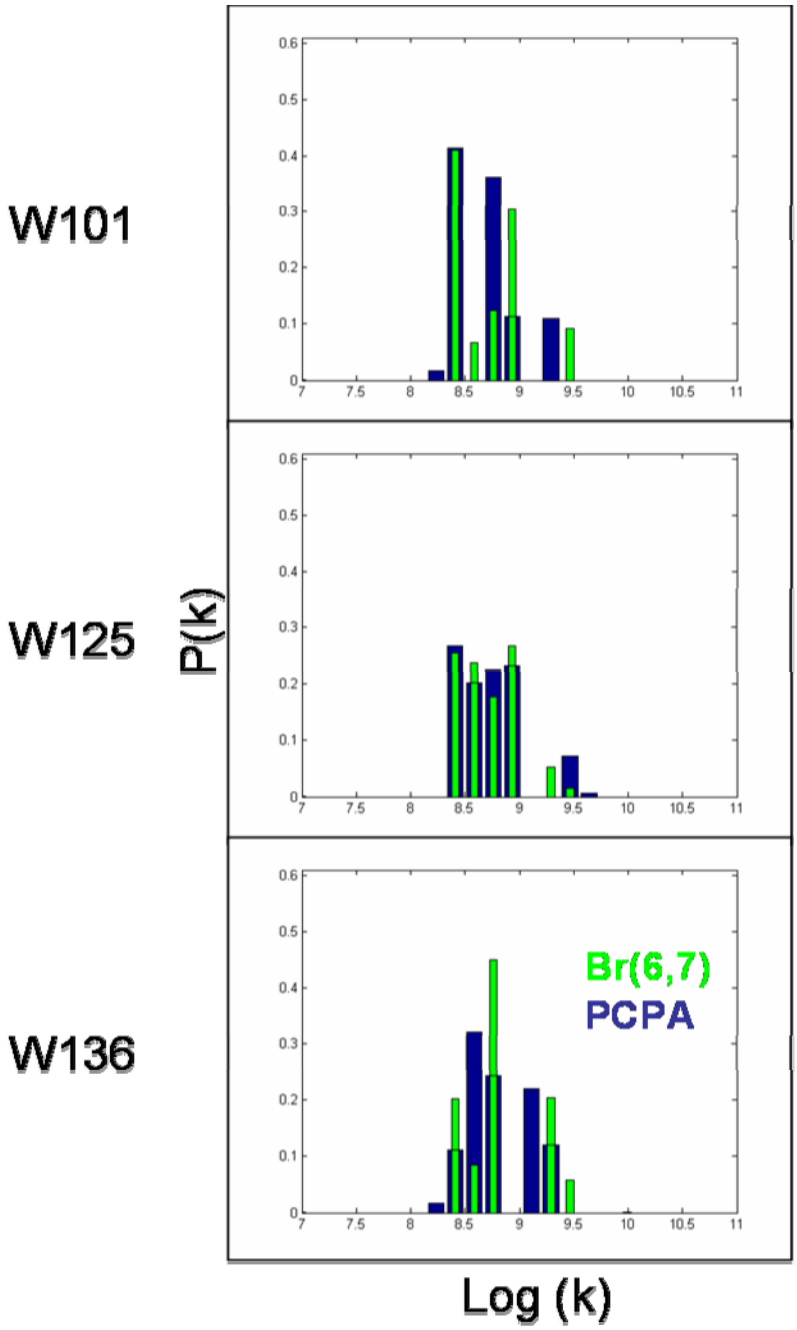

Figure 2.6. Distributions of tryptophan decay rate constants (k) for W101(top), W125 (middle), and W136 (bottom) α-syn mutants in 1:1 POPC:POPA SUVs (dark blue) and 6,7-DiBr SUVs (green)

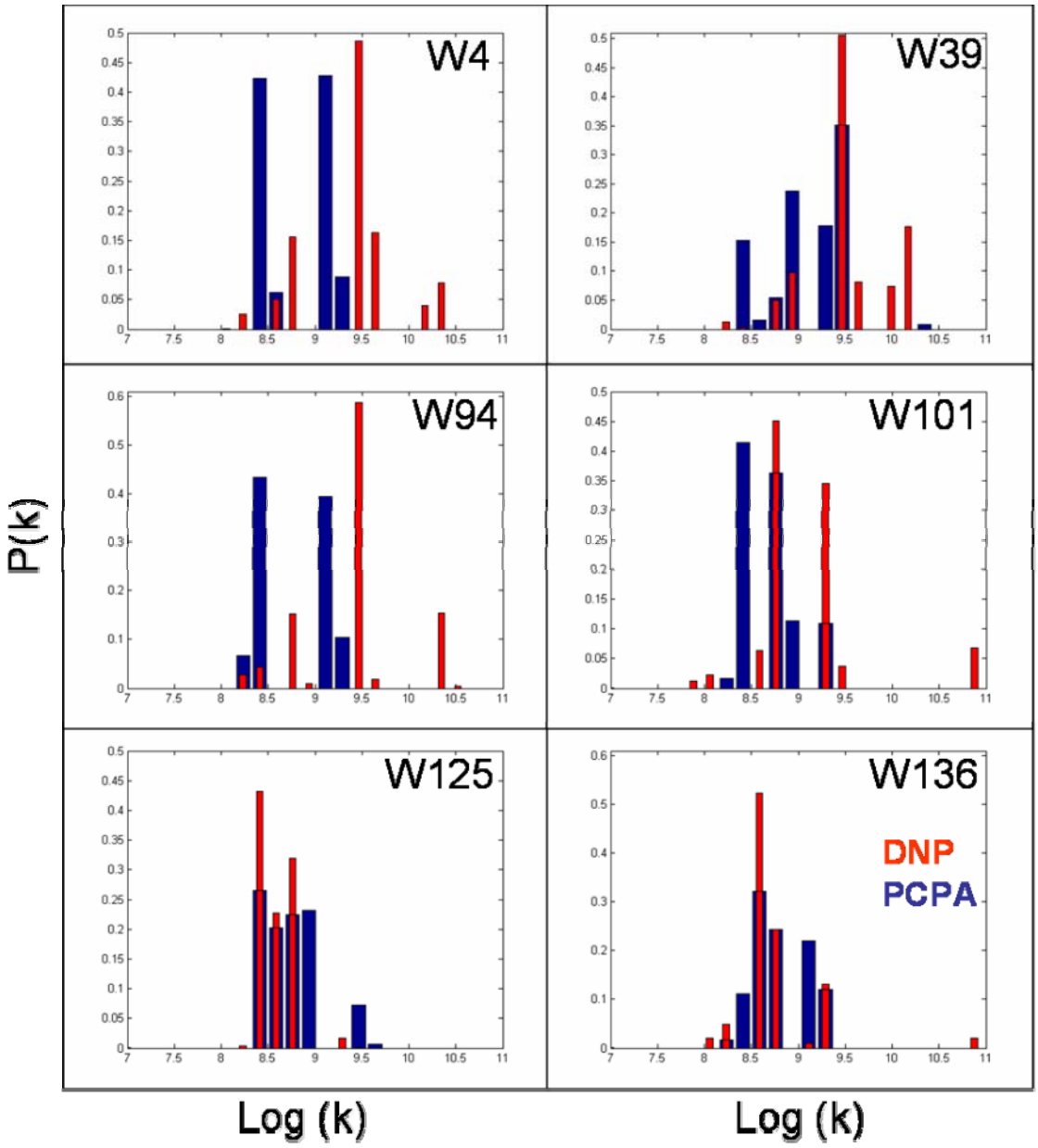

Figure 2.7. Distributions of tryptophan decay rate constants (k) for W4 (top left), W39 (top right), W94 (middle left), W101 (middle right), W125 (bottom left), and W136 (bottom right) α-syn mutants in the presence of 10 % DNP SUVs (red) and 1:1 POPC:POPA SUVs (dark blue)

W39 is located closest to the surface of the SUV. Notably, W4 is also the farthest away from the surface of the membrane when the protein associated with the phospholipid bilayer. Similarly, time-resolved fluorescence data obtained with brominated lipids gave the same order of proximity (W39 > W94 > W4) to the hydrocarbon core of the bilayer.

Similar experiments were performed on the C-terminal tail mutants, and the results were compared to the N-terminal tail mutants (**Figure 2.7**). The ultra-fast lifetimes observed for the N-terminal tail mutants were not present in the C-terminal tail positions, suggesting that these residues are not inserted in the interfacial region. However, the population of fast decay component (~ 1 x 10^{-9} s^{-1}) does increase, where W101 exhibits a sizable amplitude (41%) when it is associated with 10% DNP SUVs, suggesting that although it is not directly associated in the polar headgroup region, it is in close proximity to the surface (d ~ 30 Å). On the contrary, W136 shows considerably much less quenching in the ultra-fast population (14%), while W125 shows a negligible amount of quenching (2%). Along with the steady-state fluorescence results, we can deduce that W101 is located closest to the membrane surface, followed by W136 and W125.

Fluorescence Anisotropy Decay Kinetics.

Fluorescence anisotropy decay measurements were employed to characterize the Trp microenvironments and gain better understanding on the structural fluctuations during the excited-state decay.[16] **Figure 2.8** shows the fluorescence anisotropy decays and their exponential fits for the α-syn variants studied in the

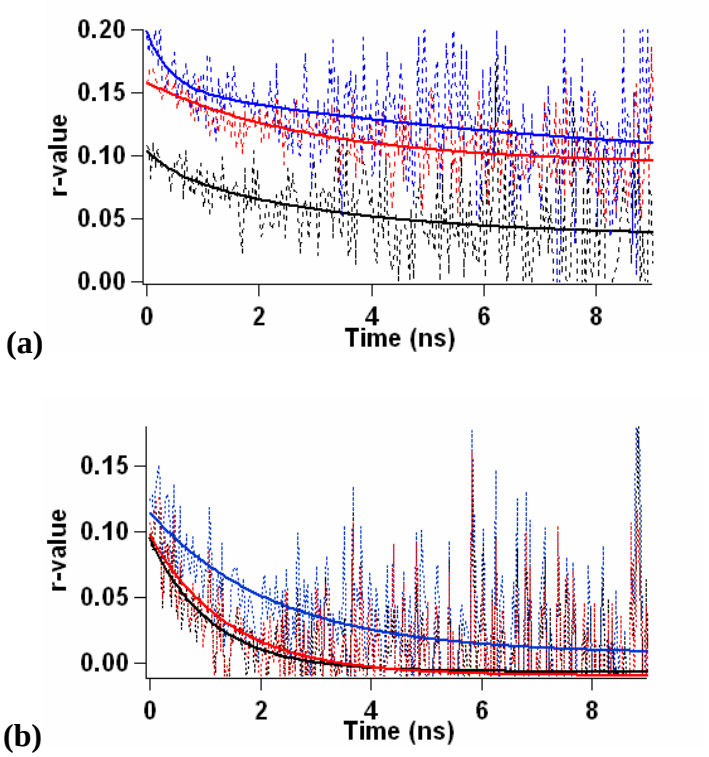

Figure 2.8. **(a)** Anisotropy decay for W4 (blue), W39 (black), and W94 (red) in 1:1 POPC:POPA SUVs. **(b)** Anisotropy decay for W101 (blue), W125 (black), and W136 (red) 1:1 POPC:POPA SUVs

presence of 1:1 POPC:POPA SUVs. Rotation correlation times (θ) were extracted from the anisotropy decays. Since rotation correlation times are related to the size and flexibility of the molecule, it is possible to draw conclusions regarding how embedded the Trp residues are in the membrane.

When α-syn is in solution, all Trp mutants demonstrate small rotation correlation times (θ ~ 1–2.5 ns). In association of SUVs, W4 has the highest rotation correlation time (θ ~ 8.3 ns). On the other hand, W39 and W94 are nearly identical θs (3.4 ns for W39 and 3.2 ns for W94). Among the C-terminal tail tryptophans, W101 has the slowest correlation time (θ ~ 2.3 ns), followed by W136 (θ ~ 1.4 ns) and W125 (θ ~ 1.1 ns). The rotation correlation times for these three mutants in solution and in vesicles show minimal increases, implying minimal insertion into the bilayer. The longest θ from W4 suggests that it is the most inserted into the membrane among the six mutants studied, followed by W94 and W39.

Other than comparing θs, anisotropy at time zero (r_0) can also be utilized to illustrate the degree of insertion of a Trp. In previous studies, it has been demonstrated that θ and r_0 increase when the rotational freedom of Trp is restricted. Kim et al. have shown that when outer membrane protein A is inserted into SUVs, the Trp's r_0 increased by approximately 50%.[16] Significant increases in θs were also demonstrated. Other studies have also shown the increase of Trp's θ when bound, such as when micelles were introduced to human apoliprotein C-I.[27] In **Figure 2.8**, it shows that W4 has the highest r_0, followed by W94 and W39. All the C-terminal tail mutants have a lower r_0 than the N-terminal mutants, with W101 showing the highest r_0 value among the three, while W125 and W136 show comparable r_0 values.

Clearly, the C-terminal Trp residues are much more flexible than the ones near the N-terminal sites. Unexpectedly, not all the C-terminal Trp data are equivalent. Our data suggest that the whole C-terminal tail is not free from influence from the membrane; in particular, in the vicinity of W101, likely through the anchoring at position 94, there is a measurable increase in local environment viscosity and polypeptide rigidity. The overall conclusions drawn from the fluorescence anisotropy measurements agree with the data collected from the other studies we performed, but differences were revealed amongst the C-terminal sites, especially in W101.

α-Syn Structure in Association with SUVs.

In summary, we can propose the following phospholipid-protein interactions illustrated in **Figure 2.9**. W39 is positioned near the surface of the SUVs, while W4 is the most inserted into the lipid bilayer among the six α-syn mutants investigated. W94 is shown to be inserted into the lipid bilayer, implying that the whole NAC region and the N-terminus participate in the α-helical structure when the protein is associated with acidic SUVs.

Since tyrosine and tryptophan both possess highly hydrophobic and hydrophilic character,[28] they are commonly found in the membrane-water interface. This phenomenon has been confirmed by this study. In fact, it has been proposed that

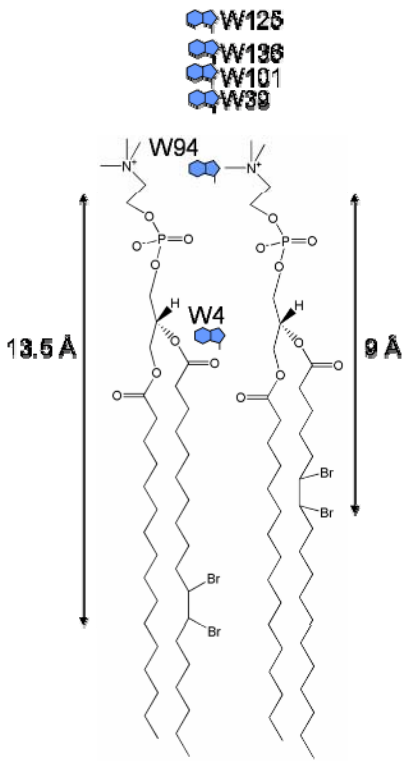

Figure 2.9. Approximate location of tryptophan residues in α-syn when associated with SUVs, drawn with respect to 11,12-DiBr (left) and 6,7-DiBr (right)

Y39 is the cause for the presence of the short linker when α-syn is associated with the membrane mimics.[11]

While the N-terminus forms a helical structure across the surface of the membrane, the C-terminal tail has been suggested to remain unstructured in the presence of acidic SUVs. Although we do agree that the C-terminal tail is not inserted in nor tightly associated to the lipid bilayer, our data suggest the possibility that W101 is in close proximity to the membrane surface and exhibits limited mobility compared to the rest of the C-terminus. This observation can be attributed to the residue being in proximity to the highly helical region.

Interestingly, we also have demonstrated that W136 has a closer interaction with the lipid bilayer than W125. It has been suggested by previous work that α-syn may possess nonrandom structure in solution.[2,3,5-7,29] Therefore, it is highly likely that the far end of the C-terminus of α-syn also has some propensity to interact closer to the membrane in the presence of acidic SUVs.

We have demonstrated that the SUVs made from lipids labeled with bromines and dinitrophenol can be used as a sensitive probe to characterize the structure of a membrane protein. Using these SUVs, we are able to assign the locations of the tryptophan residues in a phospholipid vesicle. In general, our work is in agreement with other studies conducted with NMR and EPR,[11-14] showing that the N-terminal tail of α-syn associates strongly with acidic SUVs, but does not penetrate through the membrane. On the other hand, our C-terminal tail results suggest that there could be some preferential behavior formed in that region in the presence of SUVs.

Positions for W4 and W94 when α-syn is associated with SUVs were not characterized by Langen et al. in their EPR study. They have concluded that α-syn forms three helical turns for every eleven amino acids in the region where there are seven imperfect repeats. Continuing this trend, we can postulate that W4 should be lipid exposed and W94 should be solvent exposed. Although our experimental results show that W4 is embedded into the SUV, W94 is not solvent exposed. This demonstrates that the helical property of α-syn may be contained outside of the 11-residue repeat region. On the other hand, the discrepancy observed for W94 can be attributed to the fact that the binding pattern of α-syn with membranes after residue 89 is not as structured as the repeat region.

These studies have provided additional structural insights on the folded membrane bound α-syn and serve as a foundation for future investigations. More spectroscopic studies, such as fluorescence energy transfer and dynamic contact quenching, will be employed to provide information on heterogeneous distance distributions and tertiary contacts formed in the protein, respectively.

2.5 ACKNOWLEDGEMENTS

This work was completed with Dr. Jennifer Lee's guidance.

2.6 REFERENCES

(1) Weinreb, P. H.; Zhen, W. G.; Poon, A. W.; Conway, K. A.; Lansbury, P. T. *Biochemistry* **1996**, *35*, 13709–13715.

(2) Bertoncini, C. W.; Jung, Y. S.; Fernandez, C. O.; Hoyer, W.; Griesinger, C.; Jovin, T. M.; Zweckstetter, M. *Proc. Natl. Acad. Sci. U. S. A.* **2005**, *102*, 1430–1435.

(3) Lee, J. C.; Gray, H. B.; Winkler, J. R. *J. Am. Chem. Soc.* **2005**, *127*, 16388–16389.
(4) Lee, J. C.; Langen, R.; Hummel, P. A.; Gray, H. B.; Winkler, J. R. *Proc. Natl. Acad. Sci. U. S. A.* **2004**, *101*, 16466–16471.
(5) Lee, J. C.; Lai, B. T.; Kozak, J. J.; Gray, H. B.; Winkler, J. R. *J. Phys. Chem. B* **2007**, *111*, 2107–2112.
(6) Dedmon, M. M.; Lindorff-Larsen, K.; Christodoulou, J.; Vendruscolo, M.; Dobson, C. M. *J. Am. Chem. Soc.* **2005**, *127*, 476–477.
(7) Bernado, P.; Bertoncini, C. W.; Griesinger, C.; Zweckstetter, M.; Blackledge, M. *J. Am. Chem. Soc.* **2005**, *127*, 17968–17969.
(8) Conway, K. A.; Harper, J. D.; Lansbury, P. T. *Biochemistry* **2000**, *39*, 2552–2563.
(9) Davidson, W. S.; Jonas, A.; Clayton, D. F.; George, J. M. *J. Biol. Chem.* **1998**, *273*, 9443–9449.
(10) Eliezer, D.; Kutluay, E.; Bussell, R.; Browne, G. *J. Mol. Biol.* **2001**, *307*, 1061–1073.
(11) Bussell, R.; Eliezer, D. *J. Mol. Biol.* **2003**, *329*, 763–778.
(12) Chandra, S.; Chen, X. C.; Rizo, J.; Jahn, R.; Sudhof, T. C. *J. Biol. Chem.* **2003**, *278*, 15313–15318.
(13) Ramakrishnan, M.; Jensen, P. H.; Marsh, D. *Biochemistry* **2003**, *42*, 12919–12926.
(14) Jao, C. C.; Der-Sarkissian, A.; Chen, J.; Langen, R. *Proc. Natl. Acad. Sci. U. S. A.* **2004**, *101*, 8331–8336.
(15) Ulmer, T. S.; Bax, A.; Cole, N. B.; Nussbaum, R. L. *J. Biol. Chem.* **2005**, *280*, 9595–9603.
(16) Kim, J. E.; Arjara, G.; Richards, J. H.; Gray, H. B.; Winkler, J. R. *J. Phys. Chem. B* **2006**, *110*, 17656–17662.
(17) McIntosh, T. J.; Holloway, P. W. *Biochemistry* **1987**, *26*, 1783–1788.
(18) Jakes, R.; Spillantini, M. G.; Goedert, M. *FEBS Letters* **1994**, *345*, 27–32.
(19) Winkler, G. R.; Harkins, S. B.; Lee, J. C.; Gray, H. B. *J. Phys. Chem. B* **2006**, *110*, 7058–7061.
(20) Reshetnyak, Y. K.; Koshevnik, Y.; Burstein, E. A. *Biophys. J.* **2001**, *81*, 1735–1758.
(21) Kleinschmidt, J. H.; den Blaauwen, T.; Driessen, A. J. M.; Tamm, L. K. *Biochemistry* **1999**, *38*, 5006–5016.
(22) Doring, K.; Konermann, L.; Surrey, T.; Jahnig, F. *Eur. Biophys. J.* **1995**, *23*, 423–432.
(23) Surrey, T.; Jahnig, F. *Proc. Natl. Acad. Sci. U. S. A.* **1992**, *89*, 7457–7461.
(24) Bolen, E. J.; Holloway, P. W. *Biochemistry* **1990**, *29*, 9638–9643.
(25) Narayanan, V.; Scarlata, S. *Biochemistry* **2001**, *40*, 9927–9934.
(26) Lee, H. J.; Choi, C.; Lee, S. J. *J. Biol. Chem.* **2002**, *277*, 671–678.
(27) Jonas, A.; Privat, J. P.; Wahl, P.; Osborne, J. C. *Biochemistry* **1982**, *21*, 6205–6211.
(28) Killian, J. A.; von Heijne, G. *Trends Biochem. Sci.* **2000**, *25*, 429–434.
(29) Lee, J. C.; Gray, H. B.; Langen, R.; Winkler, J. R. *Biophys. J.* **2004**, *86*, 268A-268A.